The fission yeast SPB component Cut12 links bipolar spindle formation to mitotic control

Alan J. Bridge, Mary Morphew,[1] Rachel Bartlett,[2] and Iain M. Hagan[3]

School of Biological Sciences, University of Manchester, Manchester, M13 9PT UK; [1]Department of Molecular, Cellular, and Developmental Biology, University of Colorado, Boulder, Colorado 80309-0347 USA; [2]Imperial Cancer Research Fund (ICRF), London, WC2A 3PX UK.

During fission yeast mitosis, the duplicated spindle pole bodies (SPBs) nucleate microtubule arrays that interdigitate to form the mitotic spindle. *cut12.1* mutants form a monopolar mitotic spindle, chromosome segregation fails, and the mutant undergoes a lethal cytokinesis. The *cut12*+ gene encodes a novel 62-kD protein with two predicted coiled coil regions, and one consensus phosphorylation site for $p34^{cdc2}$ and two for MAP kinase. Cut12 is localized to the SPB throughout the cell cycle, predominantly around the inner face of the interphase SPB, adjacent to the nucleus. *cut12*+ is allelic to *stf1*+; *stf1.1* is a gain-of-function mutation bypassing the requirement for the Cdc25 tyrosine phosphatase, which normally dephosphorylates and activates the $p34^{cdc2}$/cyclin B kinase to promote the onset of mitosis. Expressing a *cut12*+ cDNA carrying the *stf1.1* mutation also suppressed *cdc25.22*. The spindle defect in *cut12.1* is exacerbated by the *cdc25.22* mutation, and *stf1.1* cells formed defective spindles in a *cdc25.22* background at high temperatures. We propose that Cut12 may be a regulator or substrate of the $p34^{cdc2}$ mitotic kinase.

[*Key Words:* Mitosis; SPB; cut12; cdc25; MPF; *S. pombe*]

Microtubule organizing centers (MTOCs) play a key role in nucleating microtubule assembly and organizing existing microtubules during the formation of a bipolar mitotic spindle (Kalt and Schliwa 1993). The onset of mitosis is preceded by MTOC duplication and maturation (Balczon 1996). Mitotic onset is accompanied by the nucleation of an increased number of highly dynamic microtubules from the MTOCs (Kirschner and Mitchison 1986; Hyman and Karsenti 1996). The increase in both the number and dynamics of microtubules nucleated by the MTOC is ultimately controlled by mitosis promoting factor (MPF), a dimer consisting of the $p34^{cdc2}$ kinase subunit and a mitotic B-type cyclin (Nurse 1990). A fraction of cellular MPF has been localized to the MTOCs of organisms as diverse as yeast and man (Alfa et al. 1990; Bailly et al. 1989, 1992; Pines and Hunter 1991; Buendia et al. 1992; Maldonado-Codina and Glover 1992; Ohta et al. 1993; Pockwinse et al. 1997). The MPF component of *Xenopus* egg extracts is capable of indirectly activating the spindle microtubule nucleation capacity of the interphase spindle pole body (SPB) of permeabilized fission yeast cells (Masuda et al. 1992), and induces the increase in microtubule dynamics in vitro which is characteristic of the mitotic state (Belmont et al. 1990; Verde et al. 1990, 1992). The mitotic $p34^{cdc2}$ kinase may promote bipolar spindle formation by directly phosphorylating and activating components of the spindle apparatus such as mitotic microtubule based motor proteins (Blangy et al. 1995). Alternately, $p34^{cdc2}$ may phosphorylate and activate other kinases required for spindle formation, such as the NIMA (never in mitosis) kinase in *Aspergillus nidulans* (Ye et al. 1995). NIMA activity is essential for progression into mitosis even in the presence of active $p34^{cdc2}$/cyclin B, and NIMA is phosphorylated and stimulated by $p34^{cdc2}$ dependent phosphorylation in vitro (Ye et al. 1995, 1996). Thus, NIMA may act downstream of $p34^{cdc2}$ to promote spindle formation at the onset of mitosis. In addition to $p34^{cdc2}$ and the NIMA kinase, a family of conserved kinases termed the Polo-like kinases (Plks) play an essential role in bipolar spindle formation in a range of different eukaryotes (Glover et al. 1996). A human Plk is required for MTOC maturation (Lane and Nigg 1996) and a *Xenopus* Plk can phosphorylate and activate the MPF activator Cdc25 (Kumagai and Dunphy 1996). Thus, the Plks may act to promote the activation of $p34^{cdc2}$ kinase and spindle formation upon maturation of the duplicated MTOCs (Lane and Nigg 1996).

The rapid changes in the organization of the microtubule cytoskeleton in *Schizosaccharomyces pombe* that accompany entry into mitosis are similar to those seen in higher eukaryotes and make the fission yeast an excellent model system for the study of mitotic spindle

[3]Corresponding author.
E-MAIL Iain.Hagan@man.ac.uk; FAX 44 161 275 5082.

formation (Tanaka and Kanbe 1986; Hagan and Hyams 1988; Ding et al. 1993; Hagan and Yanagida 1997; Saito et al. 1997). Like its higher eukaryotic equivalent, the centrosome, the fission yeast SPB is excluded from the nucleus during interphase (Ding et al. 1997). In prophase, the duplicated SPBs gain access to the chromosomes through a restricted opening of the nuclear envelope and begin to nucleate spindle microtubules (Ding et al. 1997). At the onset of anaphase, the spindle microtubules decrease in number as they increase in length, and the opening in the nuclear envelope adjacent to the SPB begins to close (Ding et al. 1993, 1997). After anaphase, spindle microtubules disassemble, the SPB returns to the cytoplasm, and cytoplasmic microtubule arrays are reestablished from MTOCs at the cell equator (Hagan and Hyams 1988; Horio et al. 1991; Pichova et al. 1995) and from the outer face of the SPB (Hagan and Yanagida 1997).

Here we report the characterization of the *cut12⁺* spindle formation gene and its product. In the temperature sensitive *cut12.1* mutant only one of the two structures recognized by SPB specific antibodies nucleates microtubules, leading to monopolar spindle formation and asymmetric chromosome segregation. The *cut12⁺* gene encodes a novel 62-kD protein that is essential for bipolar spindle formation and localizes to the SPB throughout the cell cycle. The *cut12⁺* locus is allelic to a previously identified mutation termed *stf1.1* for suppressor of cdc twenty-five (Hudson et al. 1990). *stf1.1* is a semidominant mutation that bypasses the requirement for Cdc25, a normally essential tyrosine phosphatase that removes an inhibitory phosphate from p34^{cdc2} (Hudson et al. 1990). We discuss the implications of these findings for spindle formation and cell cycle control.

Results

Isolation and characterization of the cut12.1 *mutant*

A screen for temperature-sensitive mutants that increase in ploidy at the restrictive temperature has identified several mitotic mutants that undergo asymmetric chromosome segregation such as the temperature-sensitive mutant *cut12.1* (Broek et al. 1991; Hayles et al. 1994; A.M. Poziemba, A. Woollard, R.A. Craven, P. Nurse, and I. Hagan, unpubl.). To determine the precise nature of the defect in *cut12.1* an asynchronous culture of *cut12.1* was shifted from 25°C to the restrictive temperature of 36°C and stained with antibodies against the SPB component Sad1 (Hagan and Yanagida 1995) and tubulin (Woods et al. 1989). At 36°C, the *cut12.1* mutant entered mitosis but formed defective mitotic spindles. Although two Sad1 foci were often visible, only one of the two presumptive SPBs in each cell retained all the functions necessary to nucleate microtubules (Fig. 1, cells 1 and 2). The inactive Sad1 focus stained less intensely, and in extreme cases, microtubules arose from a point devoid of Sad1 (Fig. 1, cell 2). The differential staining of the two Sad1 foci is illustrated most clearly in a merged false color immunofluorescence image (Fig. 1g). Hence, the spindles formed in the *cut12.1* mutant were monopolar,

and the condensed chromatin remained in a single unsegregated mass. In spite of this defect, cells proceeded through cytokinesis, a so-called cut division, generating aneuploid (Fig. 1, cell 3) and diploid cells (Fig. 1, cell 4). As the Sad1 foci were inactive, they were randomly segregated by the central cut division.

To examine the phenotype of the *cut12.1* mutant in more detail, an early G₂ population of *cut12.1* cells was isolated at 25°C by lactose gradient centrifugation, and an aliquot was shifted to 36°C before samples were taken every 20 min for 6 hr for immunofluorescence. The population of cells entered a synchronous mitosis at both permissive and restrictive temperature, but formed monopolar mitotic spindles at the restrictive temperature and underwent cut divisions. The relative timing of appearance of these phenotypes is shown in Figure 1h. The loss of viability of the *cut12.1* mutant on shift to the restrictive temperature preceded the appearance of defective spindles and cut divisions, indicating that the defect in *cut12.1* is not reversible or that the Cut12 protein is required in some process prior to spindle formation.

Cloning and sequence analysis of the cut12⁺ *gene*

The construction of a heterozygous *cut12⁺/cut12.1* diploid showed that *cut12.1* is a recessive mutation (data not shown). The *cut12⁺* gene was therefore cloned by complementation of the temperature-sensitive defect (Fig. 2a). The *cut12⁺* gene encoded a 548 amino acid protein of 62 kD, with no overall homology to known proteins (Fig. 2b). The protein was found to be relatively hydrophilic and basic (pI of 9.4). Two regions (from amino acids 259 to 311 and 521 to 548) were predicted to form coiled coils according to the algorithm of Lupas et al. (1991). Amino acids 61–64 represented a potential phosphorylation target site for p34^{cdc2} kinase (TPLK; Nigg 1993), which also matched one of the two proposed MPM2 kinase consensus sites (LTPLK; Westendorf et al. 1994). Two potential MAP kinase phosphorylation sites from amino acids 73–76 (LKTP) and 516–519 (LKSP) were also identified (Nigg 1993). The *cut12.1* mutation is a single base change in the first nucleotide of codon 536 (CGA to TGA), which would be predicted to produce a truncated form of Cut12 lacking the carboxy-terminal 13 amino acids of the protein. As the minimum length required for the formation of a stable coiled coil is thought to be 28 amino acids (Lupas et al. 1991), the *cut12.1* allele would be predicted to encode a protein lacking a coiled coil domain at its carboxyl terminus (Fig. 2c).

cut12⁺ *gene deletion results in defective spindles and cut divisions*

The formation of monopolar spindles in the *cut12.1* mutant may be caused by the presence of sufficient Cut12 activity to allow activation of one of the two SPBs. Therefore, we examined the effect of a complete loss of Cut12 protein. One copy of the *cut12⁺* gene was deleted in a diploid by replacing all of the coding region between the *Ppu10I* sites (Fig. 2b) with the *ura4⁺* sequence of *S.*
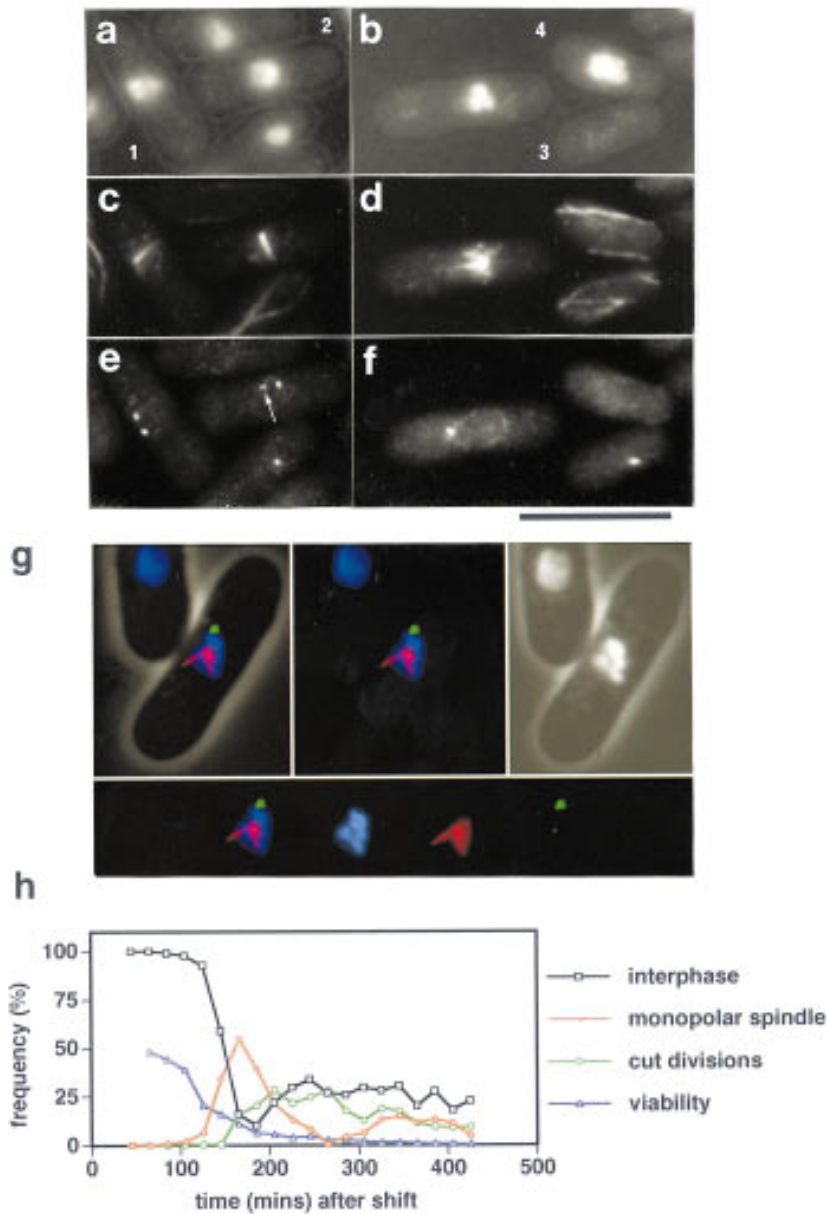
Figure 1. Monopolar mitotic spindle formation in the *cut12.1* mutant. (*a–f*) Immunofluorescence analysis of an asynchronous culture of the *cut12.1* mutant at restrictive temperature of 36°C. (*a,b*) phase/DAPI reveals cell outline and chromatin; (*c,d*) anti-tubulin staining; (*e,f*) anti-Sad1 staining. Monopolar mitotic spindles arose from one of the two foci of Sad1 staining (cells 1 and 2). The microtubules normally arose from the less bright staining of the two Sad1 foci (indicated by an arrow in cell 2). Asymmetric segregation of the chromatin and Sad1 staining material led to the formation of aneuploid cells containing Sad1 (cell 3) and diploid cells that lack any detectable Sad1 staining (cell 4). Scale bar, 10 μm. (*g*) False color immunofluorescence image of a defective monopolar spindle in the *cut12.1* mutant. Microtubules are shown in red, Sad1 staining in green, and chromatin in blue. (*Top left*) Merged image reveals cell outline and spindle structures; (*top middle*) spindle structure alone; (*top right*) phase/DAPI staining; (*bottom*) individual spindle components. The microtubules arose from the less bright staining focus of Sad1 staining. (*h*) Time course of the loss of viability and the appearance of monopolar spindles and *cut* divisions in a population of the *cut12.1* mutant grown at 25°C, synchronized in early G_2 by lactose gradient centrifugation, and then shifted to 36°C. Note that the loss of viability precedes the appearance of defective spindles and cut divisions.

pombe, thereby removing all save the first 32 nucleotides of the gene and an additional 41 nucleotides downstream of the gene. Tetrad analysis demonstrated that the *cut12*[+] gene is essential for viability at all temperatures tested from 20°C to 36°C (data not shown).

The cellular phenotypes resulting from deletion of *cut12*[+] were examined by spore germination (Fig. 3a–c). Germinating Ura[+] spores entered mitosis and disassembled cytoplasmic microtubules and condensed their chromosomes. However, the *cut12.d1* spores formed defective mitotic spindles in which microtubules were not associated with either of the two equally intense Sad1 foci. The position of the origin of spindle microtubules is indicated by an arrow in each of the three cells in Figure 3c, and clearly does not correlate with the position of the Sad1 staining foci.

We also examined the effect of a loss of Cut12 protein from a culture of the *cut12.d1* haploid in which the cells were maintained in a viable state by the expression of the *cut12*[+] cDNA from the pREP81 plasmid. The pREP81 plasmid carries an attenuated form of the thiamine repressible *nmt1*[+] promoter (Basi et al. 1993; Maundrell 1993). The repression of *cut12*[+] transcription by the addition of 2 μM thiamine resulted in the formation of defective monopolar spindles identical with those seen in the *ts cut12.1* mutant, where the microtubules arose from the less intense of the two foci of Sad1 staining (Fig. 3e,g,i). In control cultures expressing *cut12*[+], bipolar spindle formation was normal (Fig. 3d,f,h). Cells that formed defective spindles and underwent defective cut divisions were elongated relative to cells in which *cut12*[+] expression was not repressed (mean cell length
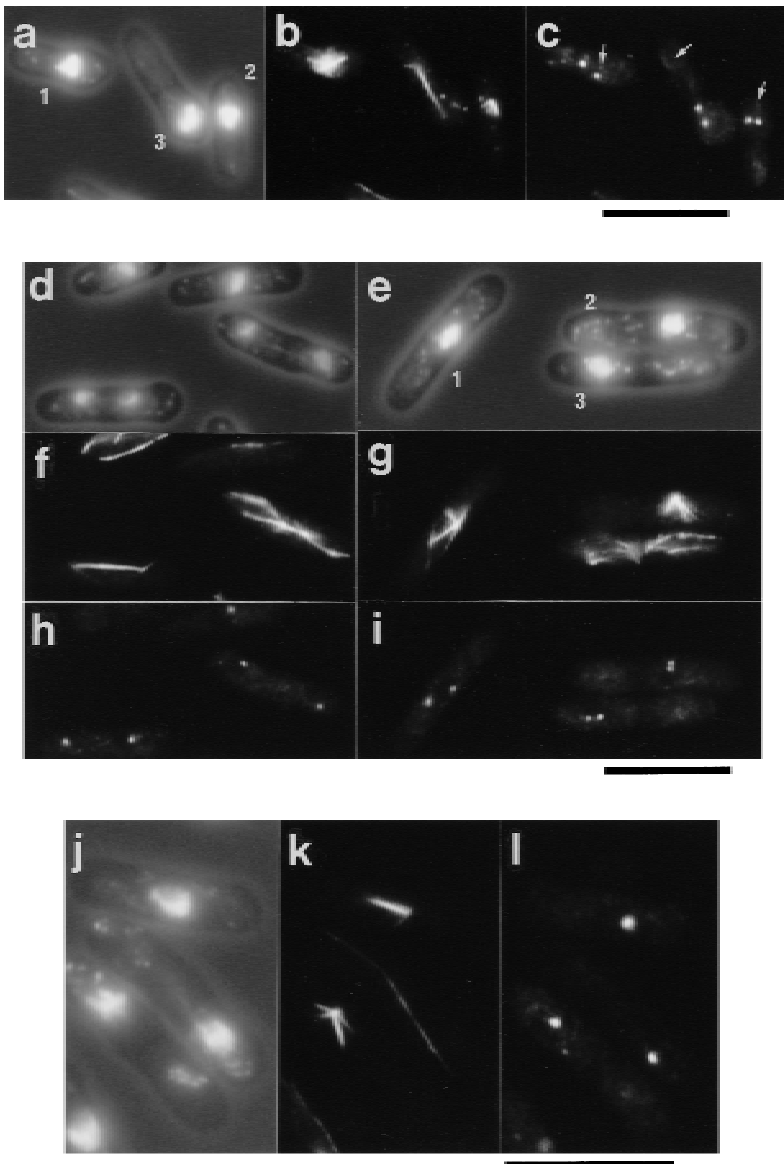
Figure 2. Cloning and molecular analysis of the *cut12*⁺ gene. (*a*) Restriction mapping and complementation analysis of the *cut12*⁺ containing clones isolated by complementation of the *cut12.1* mutant, and of subclones generated from the overlapping 2.8-kb region found in all *cut12.1* complementing plasmids. (*b*) Nucleotide and predicted amino acid sequence of the *cut12*⁺ gene. The *cut12*⁺ gene contained 2 exons of 7 and 1637 nucleotides, which together encode a predicted 548 amino acid protein of 62 kD. The two exons are separated by an intron of 42 bp; the consensus intron splice and branch sequences are shown underlined and in italics. The two regions of the Cut12 protein predicted to form coiled coils are underlined. The potential p34^{cdc2} and MAP kinase consensus sites are indicated in boldface type. (G+) The site of the *stf1.1* mutation at glycine 71. The GenBank accession no. for the *cut12*⁺ sequence is Y16837. (*c*) Predicted coiled–coil regions in the Cut12 protein were determined by applying the algorithm of Lupas et al. (1991) with a 28 amino acid window. (*d*) Schematic representation of the main features of the Cut12 protein. (+) p34^{cdc2} kinase consensus site; (star) MAP kinase consensus site; (hatched region) predicted region of coiled coil.

Figure 3. Defective spindle formation in cells deleted for the *cut12⁺* gene and cells overexpressing *cut12⁺*. (*a–c*) Defective spindle formation and cut divisions in germinating *cut12.d1* spores. Haploid spores prepared from a *cut12⁺/cut12.d1* diploid were germinated in minimal medium lacking uracil at 30°C and processed for immunofluorescence from 12 to 22 hr after inoculation. Shown are three cells fixed 16 hr after inoculation. (*A*) Phase/DAPI reveals cell outline and chromatin; (*B*) anti-tubulin staining; (*C*) anti-Sad1 staining. Germinating *cut12.d1* spores appeared to contain two foci of Sad1 staining, although the microtubules arose from a position distal to both foci, indicated by an arrow for each of the three cells. Cells also underwent *cut* divisions (cell 3). Scale bar, 10 µm. (*d–i*) Monopolar spindle formation and cut divisions following the switch off of plasmid borne *cut12⁺* expression in *cut12.d1* haploid cells. A culture of the *cut12.d1* haploid maintained by the expression of a plasmid borne copy of the *cut12⁺* cDNA from the attenuated thiamine repressible *nmt1⁺* promoter was grown to log phase in minimal medium in the absence of thiamine at 30°C. Aliquots were then inoculated into thiamine-free media to allow continued expression of *cut12⁺*, and a second aliquot inoculated into medium containing thiamine to repress *cut12⁺* expression. Samples were processed for immunofluorescence from 14 to 28 hr later. (*d,f,h*) *cut12⁺* expressed; (*e,g,i*) *cut12⁺* repressed. (*d,e*) Phase/DAPI reveals cell outline and chromatin staining; (*f,g*) anti-tubulin staining; (*h,i*) anti-Sad1 staining. Defective spindles formed in cells ~14 hr after repression of *cut12⁺*. Monopolar spindles arose from only one of the two Sad1 foci (cell 1 and 2), similar to the *ts cut12.1* mutant, and Cut divisions occurred (cell 3). Scale bar, 10 µm. (*j–l*) Immunofluorescence analysis of cells overexpressing *cut12⁺*. Cells carrying the *cut12⁺* cDNA linked to the wild-type *nmt1⁺* promoter of the pREP1 plasmid were grown to mid log phase, the culture was divided in two, and *cut12⁺* expression was derepressed in one half. Samples were taken every hour from 12 to 20 hr following induction. Shown are cells in which *cut12⁺* was derepressed for 16 hr. (*j*) Phase contrast/DAPI stain; (*k*) anti-tubulin staining; (*l*) anti-Sad1 staining. Cells overexpressing the *cut12⁺* gene formed monopolar spindles that seemed to arise from the single focus of Sad1 staining visible within the cell. Cells in which *cut12⁺* expression was repressed formed normal bipolar spindles (not shown). Scale bar, 10 µm.

13.5 µm S.E.M. 0.2 µm; and 12.4 µm, S.E.M. 0.1 µm, respectively; *n*=50). Thus, the spindles formed in the absence of Cut12 protein are monopolar and unable to support chromosome segregation, because of a defect in SPB duplication and/or activation or maturation.

cut12⁺ overexpression perturbs bipolar spindle formation

Bipolar spindle formation and cytokinesis were normal when *cut12⁺* expression from the wild-type *nmt1⁺* promoter (Maundrell 1993) was repressed (data not shown), whereas on derepression, V-shaped spindles arising from the single focus of Sad1 staining accumulated (Fig. 3j–l). A similar phenotype has been described for mutations in the kinesin-related gene *cut7⁺* (Hagan and Yanagida 1990) and the *S. pombe* Plk encoded by the *plo1⁺* gene (Ohkura et al. 1995), and may result either from a defect in SPB duplication or from the inability of cells to resolve a parallel array of microtubules to a bipolar spindle. The cells that formed monopolar spindles were elongated relative to cells in which *cut12⁺* expression was repressed (14.1 µm, S.E.M. 0.2 µm, vs. 13.5 µm, S.E.M. 0.1 µm, respectively; *n*=50).

Cut12 is an SPB component

Several approaches were taken to localize the Cut12 protein. Two polyclonal rabbit antisera were raised against amino acids 33 to 548 of the Cut12 protein fused to GST.

Affinity-purified antibodies from these sera failed to recognize any bands in a protein extract prepared from germinating *cut12*[+] deletion spores (Fig. 4a, lane 1) but recognized a single band of ~62-kD by immunoblot of a wild-type *S. pombe* extract (Fig. 4a, lane 2). Overexpression of a *cut12*[+] cDNA from the wild-type *nmt1*[+] promoter resulted in an increase in the intensity of this band (Fig. 4a, lane 3), whereas replacement of the wild-type *cut12*[+] gene with a GFP-tagged version resulted in an increase in molecular mass to ~90 kD (Fig. 4a, lane 4). We conclude that p62 is the product of the *cut12*[+] gene.

Exponentially growing wild-type cells were stained with anti-Cut12 and anti-tubulin antibodies. A single spot of anti-Cut12 staining was associated with the interphase chromatin, whereas in mitotic cells two discrete spots were seen at the mitotic spindle poles, consistent with Cut12 localization to the SPB (Fig. 4b). The intensity of these spots did not vary throughout the cell cycle.

A concern with immunolocalization data is that the specificity of antibodies in fixed samples may differ from that observed by Western blot analysis, so we used two additional methods to localize the Cut12 protein. In the first approach, the wild-type *cut12*[+] gene was replaced with a version bearing the green fluorescent protein (GFP) cDNA of *Aequorea victoria* inserted at methionine 33 (Fig. 5a). The cells were viable, and formed normal spindles, although the frequency of cells with postanaphase arrays (PAAs) was approximately double that in wild-type controls type cells (not shown). One or two distinct dots of GFP fluorescence were seen per cell (Fig. 5b–e). Staining with antibodies to the Sad1 protein confirmed that GFP and Sad1 signals were coincident (Fig. 5f–h). No variation in intensity of GFP signal was detected throughout the cell cycle.

Finally, the wild-type *cut12*[+] gene was replaced with a version of the gene bearing two copies of the Pk epitope tag (Hanke et al. 1992) at methionine 33 (*S. pombe* strain IH744). Staining of cells with anti-Pk and anti-Sad1 antibodies confirmed that the Pk and Sad1 signals were coincident throughout the cell cycle (data not shown). Depolymerization of microtubules by cold shock showed that localization of Cut12 to the SPB as judged by all three procedures was independent of microtubule integrity, indicating that Cut12 is a bona fide SPB component (data not shown).

Cut12 protein localizes to the edge of the inner face of the SPB

Cut12 protein was localized by simultaneous immunogold staining of *S. pombe* strain IH744 with both monoclonal antibodies against the Pk epitope tag (5 nm gold) and polyclonal anti-Cut12 antibodies (10 nm gold). Both probes localized specifically to the periphery of the face of the cytoplasmic body of the interphase SPB (Fig. 6a). In Figure 6b–f, the relative positions of gold particles in five serial sections through a single interphase SPB are shown; the features of note in these five sections are superimposed in Figure 6g. Whereas the Cut12 epitopes were evenly distributed along the face of the SPB adjacent to the membrane, the Pk epitope was localized to only one side.

The *cut12*[+] *locus is allelic to* stf1.1

Database comparisons of the *cut12*[+] nucleotide sequence revealed 100% identity of nucleotides 450–588 downstream of the *cut12*[+] stop codon with nucleotides 1–139

Figure 4. Characterization of anti-Cut12 antibodies and immunofluorescence localization of Cut12. (*a*) Affinity-purified rabbit antibodies against amino acids 33–548 of the Cut12 protein fused to GST were used to probe Western-blotted extracts from *cut12.d1* cells (*1*), wild-type cells (*2*), cells overexpressing a full length *cut12*[+] cDNA from the *nmt1*[+] promoter (*3*), or cells in which the wild-type *cut12*[+] gene had been replaced with a version bearing the GFP tag inserted at methionine 33 of the *cut12*[+] sequence (*4*), thereby causing a shift in predicted molecular weight of the Cut12 protein from 62 to 89 kD. (*b*) Immunolocalization of the Cut12 protein through the cell cycle. Wild-type fission yeast cells were grown to mid log phase, processed for immunofluorescence, and stained with anti-Cut12 and anti-tubulin antibodies. (*Top*) Cell outline and position of chromatin as revealed by DAPI; (*middle*) anti-tubulin staining; (*bottom*) anti-Cut12 staining. (I) interphase; (P) prophase; (M) metaphase; (AA) anaphase A; (AB) anaphase B; (PAA) postanaphase array. Interphase cells were found to contain a single dot of anti-Cut12 staining associated with the interphase chromatin, whereas in mitotic cells anti-Cut12 staining was localized to the spindle poles. Scale bar, 10 μm.
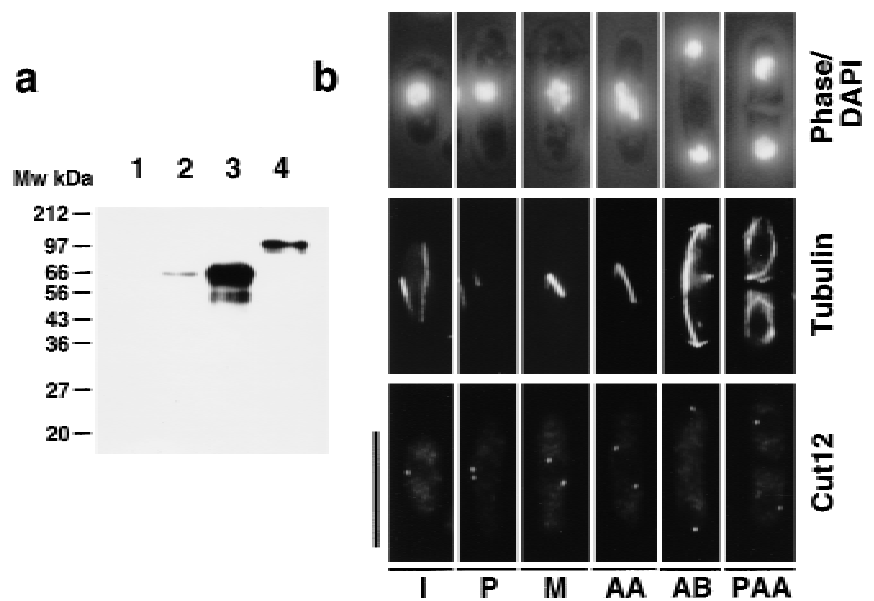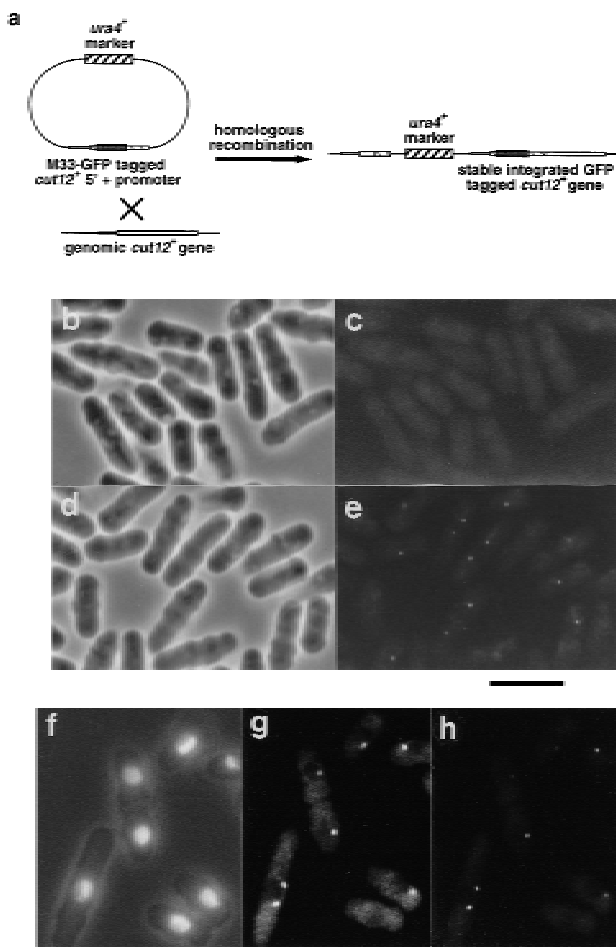
Figure 5. Localization of the Cut12 protein by use of GFP. (*a*). The wild-type *cut12*+ gene was replaced with a version bearing the GFP protein by homologous recombination with a plasmid containing the 5′ region of the *cut12*+ gene tagged at methionine 33 with the GFP cDNA. (*b–e*). Wild-type cells and cells bearing the GFP-tagged *cut12*+ gene were removed from culture and examined by phase microscopy (*b,d*) and fluorescence microscopy with standard FITC filters to reveal GFP fluorescence (*c,e*). (*b,c*) Wild-type cells; (*d,e*) Cut12-GFP tag cells. Cells carrying the integrated GFP-tagged *cut12*+ gene contained one or two dots of GFP fluorescence that were absent from wild-type cells. Scale bar, 10 μm. (*f–h*). Cells carrying integrated GFP-tagged *cut12*+ were processed for immunofluorescence and stained with anti-Sad1 antibodies. (*f*) Cell outline and chromatin revealed by DAPI; (*g*) Sad1 localization; (*h*) GFP-Cut12 localization. The GFP–Cut12 and Sad1 signals were found to colocalize in both interphase and mitotic cells. Scale bar, 10 μm.

of the *gtp1*+ gene, which encodes a putative GTP binding protein (Hudson and Young 1993). The *gtp1*+ gene was cloned by virtue of its lying immediately (449 nucleotides) downstream of the mitotic control gene *stf1*+ (Hudson et al. 1990; Hudson and Young 1993).

The *cdc25*+ gene of *S. pombe* encodes a tyrosine phosphatase that activates the p34^{cdc2}/cyclin B kinase at the G$_2$ to M transition by catalyzing the removal of inhibitory phosphorylation on tyrosine 15 of p34^{cdc2} (Russell

and Nurse 1986; Dunphy and Kumagai 1991; Gautier et al. 1991; Kumagai and Dunphy 1991; Strausfeld et al. 1991). Mutants lacking Cdc25 function replicate their DNA but fail to activate the mitotic p34^{cdc2}/cyclin B kinase, and become arrested in the G$_2$ phase of the cell cycle with an interphase array of microtubules (Russell and Nurse 1986; Hagan and Hyams 1988). *stf1.1* is a semidominant mutation that allows loss-of-function mutants in *cdc25*+, including a *cdc25*+ gene disruption, to successfully divide (Hudson et al. 1990). Our finding that both *cut12*+ and *stf1*+ appear to lie immediately upstream of the same gene indicated that the *cut12*+ and *stf1*+ genes may be identical.

We crossed a *cdc25.22* mutant in which the *cut12*+ locus was marked with the *ura4*+ gene with a *cdc25.22 stf1.1* double mutant. In 30 tetrads we found no Ura+ Cdc+ spores, corresponding to a linkage of within 1.7 cM between the Ura4+-tagged *cut12*+ locus and the *stf1.1* locus. The *cut12*+ gene was amplified from the *stf1.1* strain and the entire ORF of the PCR product sequenced directly. We identified a single base change (G–T) in codon 71 of the *cut12*+ sequence in four independent PCR reactions, which would result in the replacement of glycine 71 with a valine residue. Although expression of a plasmid borne *cut12*+ cDNA from the pREP81 plasmid was unable to rescue the *ts cdc25.22* defect, expression of the *cut12.G71V* mutant cDNA suppressed the *cdc25.22* defect at 30°C, but not at 33°C or 36°C (Fig. 7b). This level of suppression is equivalent to that seen in a *cdc25.22/cdc25.22 stf1*+*/stf1.1* diploid, which is viable up to 32°C (Hudson et al. 1990). Therefore, *cut12*+ and *stf1*+ are allelic, and a single mutation of glycine 71 to valine in *cut12*+ can suppress the requirement for Cdc25 in mitotic initiation. The *cut12.G71V* mutation did not alter the localization pattern of Cut12 as determined by immunofluorescence in either a wild-type or *cdc25.22* background at 25°C or 36°C (data not shown).

The *stf1.1 cdc25.22* mutant forms defective mitotic spindles at high temperatures

The ability of *stf1.1* to bypass the requirement for Cdc25 is incomplete. The genomic mutation *stf1.1* could suppress *cdc25.22* and a deletion of the *cdc25*+ gene only up to 35°C, whereas at 37°C, both double mutants formed small colonies that contained aberrantly dividing cells (Hudson et al. 1990). To determine the basis of the lethality at the higher temperature, the single mutants *stf1.1* and *cdc25.22,* and the double mutant *stf1.1 cdc25.22,* were grown at 25°C and shifted to 37°C. On shift to 37°C, *cdc25.22* cells arrested cell cycle progression with interphase microtubules and a single nucleus characteristic of G$_2$ (Fig. 8a,d,g) whereas *stf1.1* cells continued to form normal spindles and divide (Fig. 8b,e,h). *stf1.1 cdc25.22* cells disassembled the interphase cytoskeleton, condensed their chromosomes, and formed aberrant star shaped spindles that originated from a single large focus of Sad1 staining (Fig. 8c,f,i). The presence of an enlarged Sad1 focus caused a characteristic hole in the center of the microtubule array. Thus, whereas the *stf1.1*
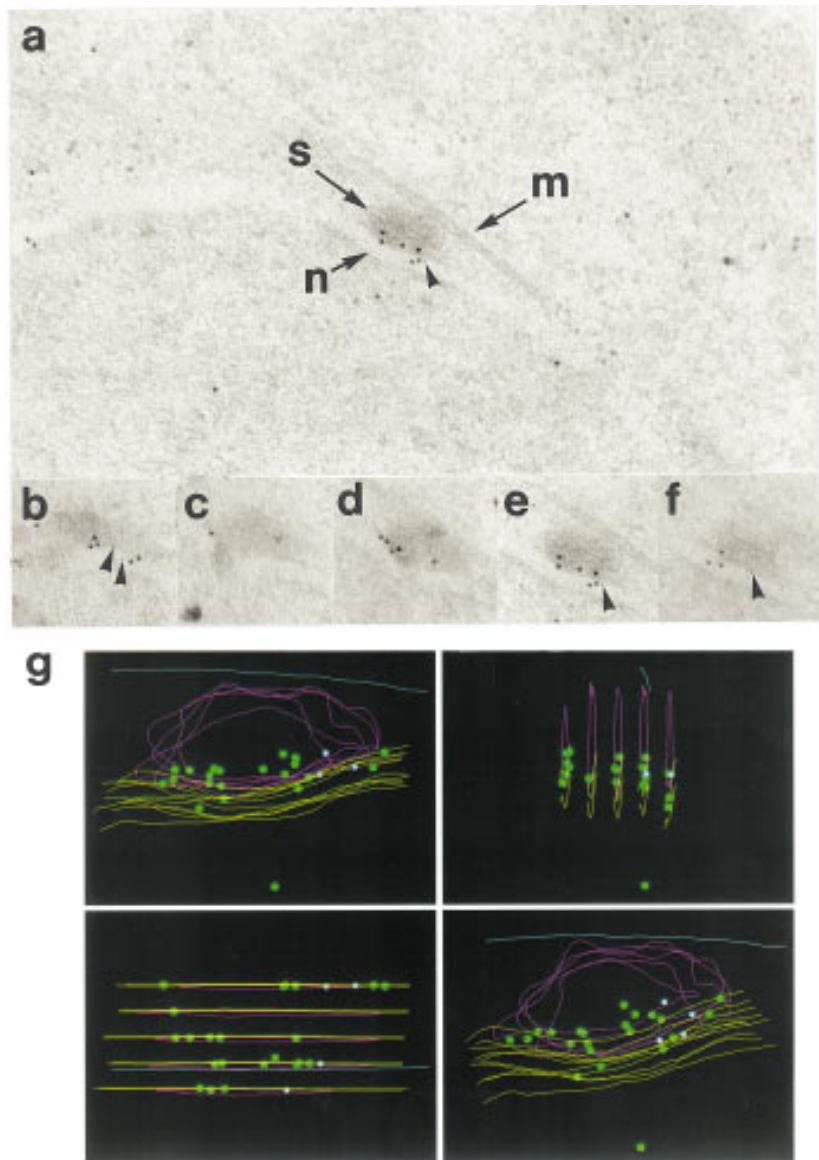
Figure 6. Electron microscopic localization of Cut12 protein within the SPB. (*a*) Immunogold staining of a section through an SPB by use of antibodies to the Pk epitope tag and a polyclonal anti-Cut12 antibody. Secondary antibodies were conjugated to gold particles of 5 nm (Pk) and 10 nm (Cut12). (S) Spindle pole body; (M) cytoplasmic microtubule laterally associated with the SPB; (N) nuclear envelope. The Cut12 epitopes were localized specifically to the inner face of the main body of the cytoplasmic SPB, adjacent to the nuclear envelope. The Pk epitope tag appeared localized more to one side of the inner face of the SPB. (*b–f*) Five serial sections through the single SPB shown in *a* were stained with antibodies to the Pk epitope tag and polyclonal antibodies to the Cut12 protein. Secondary antibodies were conjugated to gold particles of 5 nm (Pk) and 10 nm (Cut12). (*g*) Immunogold localization of Cut12 epitopes in serial sections through a single SPB in the Pk epitope tagged *cut12+* strain. The five serial sections shown in *b–f* were superimposed. (Green dots) 10 nm-gold particles (anti-Cut12); (blue dots) 5 nm gold particles (anti-Pk); (yellow lines) nuclear envelope; (red lines) SPB; (blue line) cytoplasmic microtubule.

mutation can bypass the requirement for Cdc25 at all temperatures and allow commitment to mitosis, at 37°C the spindles that are formed in the *stf1.1* mutant in the absence of Cdc25 function are defective.

cdc25.22 *exacerbates the spindle formation defect in* cut12.1

As a semidominant mutation in *cut12* can bypass the requirement for Cdc25, we determined the effect of combining the loss-of-function *cut12.1* mutation with *cdc25.22.* Although the single *cdc25.22* and *cut12.1* mutants were viable up to 30°C, the double mutant *cut12.1 cdc25.22* was viable only at 20°C and unable to grow at temperatures of 25°C and above (Fig. 9a). On shift to 25°C, the *cut12.1 cdc25.22* cells entered mitosis and formed monopolar spindles that arose from a weakly staining focus of Sad1 staining (Fig. 9b–d). This pheno-

type is identical to that of the single *cut12.1* mutant on shift from 25°C to 36°C (Fig. 1). At 36°C, the double mutant *cut12.1 cdc25.22* arrested with interphase microtubules characteristic of the G_2 arrest seen in the single mutant *cdc25.22* (data not shown). Thus, the presence of the *cdc25.22* mutation exacerbates the spindle defect in the *cut12.1* mutant.

Discussion

We have shown that loss-of-function of the SPB component Cut12 leads to the formation of defective monopolar spindles. Unexpectedly, a semidominant mutation in *cut12+* can bypass the requirement for the essential MPF activating tyrosine phosphatase Cdc25 (Hudson et al. 1990, 1991). This was suprising as Cut12 is therefore an SPB component that is both essential for bipolar spindle formation and capable of influencing the require-
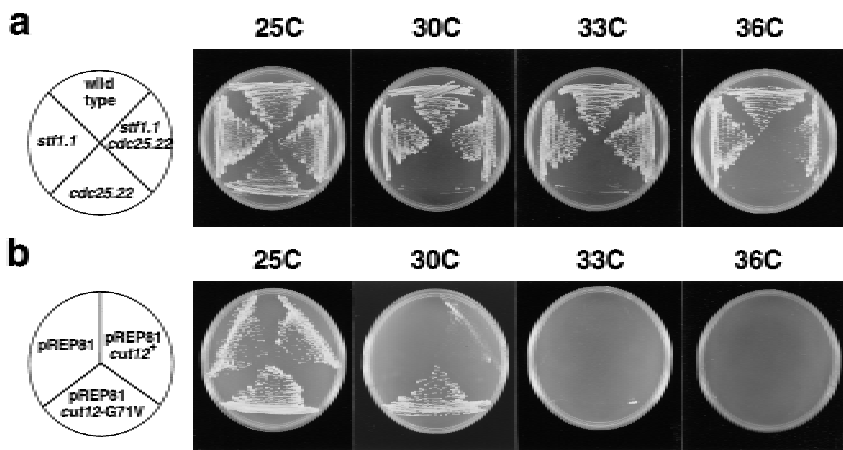
Figure 7. The *cut12*[+] and *stf1*[+] genes are identical. (*a*) Temperature sensitivity of the *cdc25.22* and *stf1.1* single mutants and a *cdc25.22 stf1.1* double mutant. Cells were streaked onto complete medium at 25°C, 30°C, 33°C, and 36°C. The *stf1.1* mutation allowed growth of a *cdc25.22* mutant on complete medium at all four temperatures tested, although at 36°C growth was slow relative to wild-type cells, and colony size is irregular. (*b*) Suppression of *cdc25.22* by a point mutation in the *cut12*[+] gene. *cdc25.22* mutant cells carrying a pREP81 plasmid containing no insert, a full-length wild-type *cut12*[+] cDNA, or the mutant *cut12.G71V* cDNA, were streaked onto minimal medium lacking thiamine at 25°C, 30°C , 33°C, and 36°C. Although *cdc25.22* cells carrying a blank plasmid or the wild-type *cut12*[+] gene were unable to form colonies at 30°C, *cdc25.22* cells carrying the *cut12.G71V* mutant cDNA were able to grow at 30°C but not 33°C. This is consistent with the ability of a *cdc25.22/cdc25.22 stf1.1/stf1*[+] diploid to grow at temperatures below 33°C (Hudson et al. 1990).

ment for a normally essential inducer of mitosis. Because the loss-of-function phenotype defines *cut12*[+] as a cut gene, whereas the *stf1.1* mutation is a gain-of-function mutation, we will refer to the *cut12*[+]/*stf1*[+] gene as *cut12*[+].

Loss of Cut12 function leads to formation of monopolar spindles

The interphase fission yeast SPB consists of two components. The main body of the SPB resides in the cytoplasm and is separated from the mitotic spindle microtubule nucleator γ-tubulin by the nuclear envelope (Ding et al. 1997). Mitotic activation of the SPB is accompanied by localized nuclear envelope breakdown and association of these two elements. In actively dividing cells that lack Cut12 function, Sad1 localization did not correlate with microtubule nucleating activity. This may indicate

that these two elements of the mitotic SPB remain independent in the absence of Cut12.

In *cut12.1,* monopolar spindles arose from the weaker of the two Sad1 staining foci, whereas in germinating *cut12.d1* spores monopolar spindles were not associated with either of the two equally staining Sad1 foci. The differential effect of the *cut12.1* mutation on the two SPBs suggests that Cut12 is incorporated into the duplicated SPBs in a conservative fashion, and that the Cut12 protein incorporated into the SPB in the cell cycle prior to the temperature shift is stabilized. Differential behavior of the duplicated SPBs is also illustrated by the activation of the cytokinesis regulating GTPase Spg1 on only one of the two anaphase SPBs (Sohrmann et al. 1998). As the two SPBs appear to be generated by fission of a larger precursor to two smaller structures (Ding et al. 1997), the nonequivalence between the two daughter
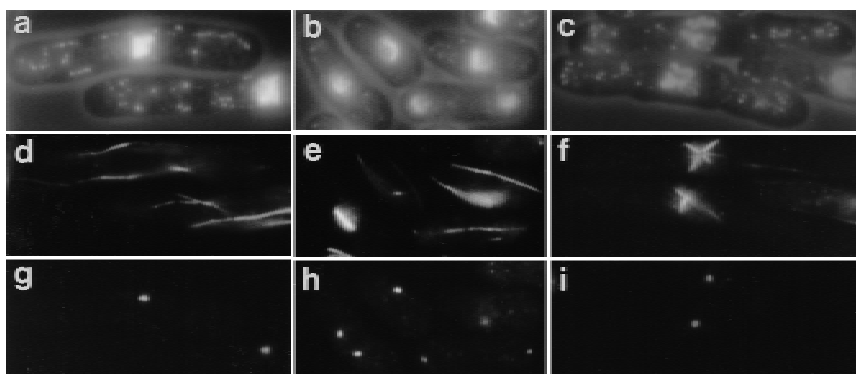

Figure 8. The *stf1.1* mutant has a temperature-sensitive spindle defect in a *cdc25.22* background. (*a–i*) Immunofluorescence analysis of the *cdc25.22* and *stf1.1* single mutants and the double mutant *cdc25.22 stf1.1.* Cells were cultured in complete medium to mid-log phase at 25°C and then shifted to 37°C, and processed for immunofluorescence analysis. (*a–c*) Phase/DAPI; (*d–f*) anti-tubulin staining; (*g–i*) anti-Sad1 staining. (*a,d,g*) *cdc25.22;* (*e,f,h*) *stf1.1;* (*c,f,i*) *cdc25.22 stf1.1.* The single *cdc25.22* mutant arrested with an interphase cytoskeleton characteristic of a G$_2$ cell, whereas the *stf1.1* mutant continued to form normal spindles and divide. The double-mutant *cdc25.22 stf1.1* formed aberrant star-shaped spindles arising from a single large Sad1 focus within the cell. Scale bar, 10 μm.
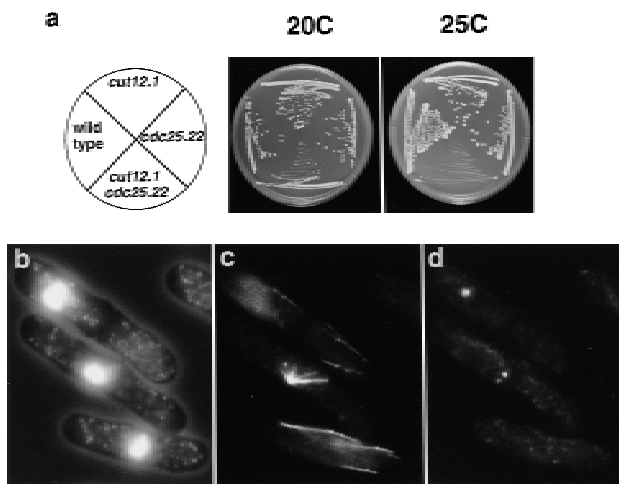
Figure 9. Synthetic lethality between *cut12.1* and *cdc25.22*. (*a*) Temperature sensitivity of *cdc25.22, cut12.1,* and *cdc25.22 cut12.1* mutants. Cells were streaked onto complete medium at 20°C and 25°C. Although the single mutants *cdc25.22* and *cut12.1* both grew at 25°C, the double mutant *cdc25.22 cut12.1* was inviable at this temperature. (*b–d*) Immunofluorescence analysis of phenotype of the *cdc25.22 cut12.1* mutants. Cells were cultured in complete medium at 20°C and then shifted to 25°C and processed for immunofluorescence. (*b*) Cell outline and chromatin; (*c*) anti-tubulin staining; (*d*) anti-Sad1 staining. On shift to 25°C, the *cdc25.22 cut12.1* mutant formed defective spindles. Although the *cdc25.22 cut12.1* cells appeared to contain two foci of Sad1 staining, cells formed defective monopolar spindles that arose from the less bright staining Sad1 focus, as in the *cut12.1* mutant at 36°C. Scale bar, 10 μm.

SPBs may be generated by localized incorporation of new material within a particular region of the SPB during growth; fission would then lead to the production of a mature and a new SPB. The apparent asymmetry of exposure of amino-terminal epitopes of Cut12 within the SPB supports this possibility.

cut12.G71V *bypasses the requirement for Cdc25*

The p34^{cdc2} kinase is subject to inhibitory phosphorylation on T14 and Y15 residues, and the removal of these inhibitory phosphates determines the timing of entry into mitosis (Gould and Nurse 1989). In fission yeast this inhibitory phosphorylation is catalyzed in by the Wee1 kinase and a redundant Wee1 homolog Mik1 (Russell and Nurse 1987a; Featherstone and Russell 1991; Lundgren et al. 1991; Parker et al. 1993; Lee et al. 1994; Den Haese et al. 1995). The action of the Wee1/Mik1 kinases is opposed by Cdc25 phosphatase (Fantes 1979; Russell and Nurse 1986), which dephosphorylates both T14 and Y15 in vitro (Dunphy and Kumagai 1991; Gautier et al. 1991; Kumagai and Dunphy 1991; Strausfeld et al. 1991).

The activity of Cdc25 is stimulated by cell-cycle specific phosphorylation of certain sites (Ducommun et al. 1990; Moreno et al. 1990; Izumi et al. 1992; Kumagai and Dunphy 1992; Hoffmann et al. 1993; Izumi and Maller

1993). The Wee1 and Mik1 kinases are also subject to cell cycle-dependent phosphorylation that has been reported to inhibit the activity of the kinase (Russell and Nurse 1987b; Coleman et al. 1993; Parker et al. 1993; Tang et al. 1993; Wu and Russell 1993; McGowan and Russell 1995; Mueller et al. 1995; Watanabe et al. 1995). Thus, phosphorylation of both Cdc25 and the opposing Wee1/Mik1 kinases promotes the activation of p34^{cdc2}/cyclin B and onset of mitosis. Phosphorylation and inhibition of Wee1 is catalyzed by the action of the Nim1/Cdr1 kinase (Coleman et al. 1993; Parker et al. 1993; Wu and Russell 1993), and other unrelated kinases including MPM2 epitope kinases (Tang et al. 1993; Mueller et al. 1995). The stimulatory phosphorylation of Cdc25 can be accomplished in vitro by either the p34^{cdc2}/cyclin B kinase (Hoffmann et al. 1993; Izumi and Maller 1993) or by non-p34^{cdc2} kinases including MPM2 epitope kinases such as the *Xenopus* Plx kinase (Kuang et al. 1994; Izumi and Maller 1995; Kumagai and Dunphy 1996). Biochemical studies in *Xenopus* have demonstrated the existence of a positive feedback loop involving p34^{cdc2} and Cdc25, in which Cdc25 may dephosphorylate and activate p34^{cdc2}/cyclin B, which then phosphorylates and stimulates Cdc25 to, in turn, dephosphorylate further p34^{cdc2}/cyclin B, leading to the rapid amplification of a small quantity of MPF and entry into mitosis (Izumi and Maller 1993; Hoffmann et al. 1993). This amplification loop could be triggered by the p34^{cdc2} independent phosphorylation and activation of Cdc25, or by the phosphorylation and inhibition of Wee1/Mik1. The loop may also be triggered by the generation of a fraction of p34^{cdc2}/cyclin B that does not require Cdc25 for activation or that is not sensitive to inhibition by Wee1/Mik1.

Within this context, a number of models can be considered that may account for the ability of a semidominant mutation in an SPB component to bypass the requirement for Cdc25. Cut12 is unlikely to solely regulate the activity of Cdc25, as *stf1.1* can suppress a complete loss of Cdc25 activity arising from the disruption of the *cdc25$^+$* gene (Hudson et al. 1990, 1991). Cut12 is also unlikely to solely regulate Wee1, as *stf1.1* is additive with *wee1.50* in suppression of *cdc25.22* and is sensitive to the overexpression of *wee1$^+$* (Hudson et al. 1990). Cut12 might, however, directly or indirectly regulate the activities of both Wee1 and Mik1, or possibly interact with a dual regulator of Cdc25 and Wee1/Mik1 function, a role proposed for the *Xenopus* Plx MPM2 kinase (Kumagai and Dunphy 1996; Lane and Nigg 1996). In both these models, Cut12 may promote mitosis in the absence of Cdc25 function by down-regulating both Wee1 and Mik1, thereby relieving the negative restraint that holds a *cdc25.22* mutant in G$_2$. Cut12 could also relieve this restraint by promoting Y15 dephosphorylation of p34^{cdc2} by another tyrosine phosphatase, such as the tyrosine phosphatase Pyp3 (Millar et al. 1992). Pyp3 is unrelated to Cdc25 but may act cooperatively with Cdc25 to dephosphorylate Y15 of p34^{cdc2} (Millar et al. 1992). However, the *stf1.1* mutation is unlikely to bypass loss of Cdc25 function by increasing *pyp3$^+$* activity, as loss of *pyp3$^+$* function does not appear to lead to Cut

divisions (Millar et al. 1992). In a simpler model *stf1.1* may allow the formation of p34^{cdc2}/cyclin B complexes at the SPB that are not subject to inhibition by Wee1/Mik1 kinases.

Potential interactions between Cut12 and MPF

Genetic studies in fission yeast have shown that the requirement for Cdc25 function can be altered by mutation of the *cdc2$^+$* gene and its cyclin B-type partner encoded by the *cdc13$^+$* gene. Like *cut12.G71V,* a gain-of-function mutation in *cdc2$^+$* termed *cdc2.3w* can bypass the requirement for Cdc25 activity at the G$_2$-to-M transition (Carr et al. 1989; Gould et al. 1990; MacNeill and Nurse 1993), whereas loss-of-function mutations in *cdc13$^+$* are, like *cut12.1,* synthetically lethal with *cdc25.22* (Bueno and Russell 1993). The genetic interaction between *cdc25.22* and both loss- and gain-of-function alleles in *cut12$^+$* are consistent with Cut12 acting as a regulator or substrate of the p34^{cdc2}/cyclin B kinase. Both p34^{cdc2} and Cdc13 have been localized to the SPB (Alfa et al. 1990), and mutations in the *cdc2$^+$* and *cdc13$^+$* genes have been identified that can specifically inhibit chromosome segregation but not other events of mitosis such as chromosome condensation and septation (Labib et al. 1995; Berry and Gould 1996; Gould and Feoktistova 1996). *cdc2.Y15T* and *cdc13.A381V* are perhaps particularly relevant in this regard, as these mutant proteins may be unable to promote spindle formation because of a defective interaction with a regulatory subunit that is specifically required for this process (Berry and Gould 1996; Gould and Feoktistova 1996). It has also been suggested that a higher threshold level of p34^{cdc2}/cyclin B kinase activity may be required for mitotic spindle formation than for chromosome condensation and septation, and that mutants such as *cdc2.Y15T* may be unable to attain this level of activity (Gould and Feoktistova 1996). Therefore, Cut12 may be a limiting substrate normally phosphorylated only when the p34^{cdc2}/cyclin B activity reaches the level required for bipolar spindle formation. The *cut12.G71V* mutation lies between the closely apposed amino-terminal MAP kinase and p34^{cdc2} consensus sites, and Cut12.G71V may conceivably mimic an activated form of Cut12 and allow progression through mitosis in the presence of a lower level of p34^{cdc2}/cyclin B kinase activity. Loss-of-function mutants in *cut12$^+$* undergo chromosome condensation and septation without forming a bipolar spindle. A similar phenotype to *cut12.1* is seen in mutants of *A. nidulans* that enter mitosis in the absence of NIMA function, a known mitotic substrate of p34^{cdc2}/cyclin B kinase (Osmani et al. 1991a; Ye et al. 1995). Whereas the *nimA5* mutant normally arrests in G$_2$ with duplicated SPBs and high p34^{cdc2}/cyclin B kinase activity, the *bimE7 nimA5* double mutant escapes this G$_2$ arrest and attempts an aberrant mitosis with defective SPBs (Oakley and Morris 1983; Osmani et al. 1991a,b). Thus, loss-of-function mutations in downstream effectors of p34^{cdc2} function may uncouple the normally coordinated events of mitosis such as spindle formation and chromosome condensation and septation.

Whatever the precise mechanism by which *stf1.1* bypasses the requirement for Cdc25, the demonstration that an essential component of the SPB can influence the requirement for activators of p34^{cdc2}/cyclin B highlights the importance of events at the spindle pole to cell cycle progression in general.

Materials and methods

Cell culture and strains

Cell culture and maintenance was carried out according to Moreno et al. (1991). All Cut12 localization experiments, and the analysis of spindle formation defects in *cut12.1, cut12.1 cdc25.22,* and *stf1.1 cdc25.22* mutants, were carried out on cells cultured in rich YES medium. The *cut12$^+$* deletion and overexpression analyses, plus all cell length measurements, were carried out on cells grown in Edinburgh minimal medium (EMMG) that is equivalent to EMM2 (Moreno et al. 1991) but substitutes 5 grams/liter glutamic acid for 5 grams/liter ammonium acetate as a nitrogen source. Synchronous cultures were generated by size selection of small G$_2$ cells on a lactose gradient as described previously (Hagan and Yanagida 1997). The strains used in this paper are shown in Table 1.

Isolation and sequencing of the cut12$^+$ gene

Standard DNA manipulations were carried out according to Sambrook et al. (1989). The *cut12$^+$* gene was isolated by complementation of the temperature-sensitive mutant. Fourteen transformants carrying five complementing plasmids were isolated from screens of two genomic *S. pombe* libraries (the generous gift of Dr. A. Carr; Barbet et al. 1993). These plasmids had an overlapping region of ~2.8 kb, including the minimum complementing 2.0-kb *Eco*RV–*Pvu*II fragment. Integration of a plasmid containing a portion of the cloned DNA linked to the *ura4$^+$* gene by homologous recombination showed that the cloned region contained the *cut12$^+$* gene, as no recombination was observed between the *cut12.1* and *ura4$^+$* in >1100 spores (Nurse 1975). A 1.0-kb *Hin*dIII–*Eco*RV and a 2.0-kb *Hin*dIII fragment that together completely covered this minimum complementing region were cloned into the Bluescript plasmid to generate the pSCUT12-1 and pSCUT12-2 plasmids, respectively, and nested deletions made by use of exonuclease III. DNA sequencing was performed on both strands by the manual dideoxy method with T7 DNA polymerase. The presence of the predicted 42-bp intron was confirmed by sequencing a clone isolated by PCR amplification from a pREP1 based cDNA library (a gift from Dr. C. Norbury, John Radcliffe Hospital, Institute of Molecular Medicine, ICRF, Molecular Oncology Laboratory, Oxford, UK) by use of primers (5′-TTCAGAGATCCGATAGAATGTCAG-3′) and (5′-CCTTCGTCTTCTCCTTTCCTCTAATC-3′). The *cut12.1* mutant version of the *cut12$^+$* gene was isolated by PCR amplification with two primers (5′-CGACTAATACGGCCTTTTACAAGCC-3′) and (5′-CATGCAGAACAATTCAGAGATCCG-3′). PCR products were sequenced directly by a manual T7 DNA polymerase procedure. Where a mutation was identified, that region of the gene was sequenced again from four independent PCR reactions.

Construction of the cut12.d1 deletion

A 4-kb genomic *Pst*1–*Kpn*I fragment from the shortest *cut12.1* complementing genomic clone was cloned into *Pst*1–*Kpn*I–di-

Table 1. *Strains used in this study*

Strain	Genotype	Origin
IH310	*leu1.32/leu1.32 ade6.M210/ade6.M216 ura4.d18/ura4.d18* h⁻/h⁺	lab stock
IH365	*leu1.32 ura4.d18* h⁻	lab stock
IH566	*cdc25.22 leu1.32 ura4.d18* h⁻	lab stock
IH571	*cut12.M33GFP:ura4⁺ leu1.32 ura4.d18* h⁻	this study
IH572	*cut12.dl/cut12⁺ leu1.32/leu1.32 ade6.M210/ade6.M216 ura4.d18/ura4.d18* h⁻/h⁺	this study
IH596	*cut12.1 leu1.32 ura4.d18* h⁻	this study
IH666	*stf1.1 leu1.32* h⁺	Hudson et al. (1990)
IH667	*stf1.1 cdc25.22 leu1.32 ura4.d18* h90	Hudson et al. (1990)
IH741	*stf1.1 cdc25.22 leu1.32 ura4.d18* h⁻	Hudson et al. (1990)
IH744	*cut12.M33Pk:ura4⁺ leu1.32 ura4.d18* h⁻	this study
IH751	*cdc25.22 cut12.M33Pk:ura4⁺ leu1.32 ura4.d18* h⁻	this study
IH970	*cdc25.22 leu1.32 ura4.d18 pREP81–cut12.G71V* h⁻	this study
IH972	*cdc25.22 leu1.32 ura4.d18 pREP81–cut12⁺* h⁻	this study
IH1080	*cdc25.22 leu1.32 ura4.d18 pREP81* h⁻	this study
IH1110	*cut12.d1 ade6 leu1.32 pREP81–cut12⁺* h⁻	this study
IH1120	*stf1.1 leu1.32 ura4.d18* h⁻	this study
IH1225	*leu1.32 ura4.d18 pREP1* h⁻	this study
IH1226	*leu1.32 ura4.d18 pREP1–cut12⁺* h⁻	this study
IH1227	*cut12.1/cut12⁺ leu1.32/leu1.32 ade6.M210/ade6.M216 ura4.d18/ura4.d18* h⁻/h⁺	this study

gested pUC19 to generate the plasmid pDCUT12-1. A 1.6-kb *Ppu*10I fragment containing all of the *cut12⁺* coding sequence, with the exception of the first 10 amino acids, was removed from pDCUT12-1 and replaced with a *Not*I linker (GCGGC-CGC) to generate pDCUT12-2. A 1.8-kb *Acc*III fragment containing the *ura4⁺* gene (Barbet et al. 1993) was inserted into the linker to generate pDCUT12-3. A 4-kb fragment containing the *cut12⁺* gene deleted by the *ura4⁺* gene was purified from pD-CUT12-3 and used to transform a diploid (h⁺/h⁻ *leu1-32/leu1-32 ura4-d18/ura4-d18 ade6-M210/ade6-M216*). Stable Ura⁺ diploids that had the desired replacement determined by genomic Southern hybridization were selected. Probing with a 2.0-kb *Hin*dIII fragment containing the 3′ region of the *cut12⁺* gene revealed a 3.7-kb *Bgl*II fragment in the deletion diploid in addition to the 1.7- and 2.0-kb bands observed in wild type.

Construction of a full-length cut12⁺ cDNA for overexpression studies

pREP1 and pREP81 were used to express *cut12⁺* under the control of the thiamine repressible *nmt1⁺* promoter (Basi et al. 1993; Maundrell 1993). For the construction of the *Nde*I site (CATATG) at the initiator codon, the plasmid pSCUT12-1 was digested with *Nsi*I. Two oligonucelotides (5′-ATATGT-CAGAAACTTTGAACACTCCGCCAACC-3′) and (5′-TAG-GTTGGCGGAGTGTTCAAAGTTTCTGACA-3′) were allowed to anneal to generate a linker that was inserted at the *Nsi*I site, thereby generating a clone bearing the 5′ region of *cut12⁺* gene with two copies of the *cut12⁺* start codon and the first 10 amino acids, in which the original start codon was followed by the intron, and the newly introduced second start codon had an *Nde*I site at the ATG. The original *Nde*I site at nucleotides 29–34 of the *cut12⁺* coding sequence was also removed by this procedure. The plasmid was designated pSCUT12-1/M1*Nde*I. A *Bgl*II–*Eco*RV fragment from pSCUT12-1/M1*Nde*I was subcloned back into the 4-kb genomic *cut12⁺* clone. This construct was then digested with *Nde*I and *Pvu*II, to yield a 2.2-kb fragment bearing the full length *cut12⁺* cDNA and ~300 bp 3′ of the gene. The *Nde*I–*Pvu*II fragment was then inserted into *Nde*I–*Sma*I–digested pREP plasmids.

Construction of an integrated GFP-tagged version of the cut12⁺ gene

The GFP tag was inserted at an *Nde*I site created at methionine 33 of the *cut12⁺* sequence. The pSCUT12-1 plasmid was used as a template for site directed mutagenesis by use of the primer 5′-GCCTGTTACACATATGTCCTCTTAC-3′, and the resulting mutant clone (pSCUT12-1/M33*Nde*I) was sequenced entirely between the initiator codon and the *Hin*dIII site to confirm that no errors had been introduced during the mutagenesis procedure. The GFP cDNA as an *Nde*I fragment (R. Craven, D. Griffiths, K. Sheldrick, R. Randall, I. Hagan, and A. Carr, in prep.) was then inserted into this position to give pSCUT12-1/M33GFP. To create the plasmid for integrative transformation of *cut12⁺*-GFP into the genome, the *Hin*dIII–*Eco*RV fragment was then cloned into *Hin*dIII–*Eco*RV–digested Bluescript with *ura4⁺* inserted at the *Not*I site to form pINTCUT12-1/M33GFP.

Construction of an integrated Pk epitope-tagged version of the cut12⁺ gene

For epitope tagging the *cut12⁺* gene, we used a pREP42 plasmid (pREP42-PkN) bearing three copies of the Pk epitope tag (amino acid sequence IPNPLLGLD; R. Craven, D. Griffiths, K. Sheldrick, R. Randall, I. Hagan, and A. Carr, in prep.), inserted as an *Nde*I cassette at the multicloning site. The cassette also bears an internal *Nco*I site following the second copy of the tag; hence, it is possible to link *Nco*I-digested genes to the Pk tag bearing pREP42 plasmid, and then re-excise the gene along with two copies of the Pk tag by *Nde*I digest. An *Nco*I site was inserted at M33 of the *cut12⁺* sequence by site-directed mutagenesis on the pSCUT12-1 plasmid by use of the primer 5′-GCCT-GTTACAACCATGGCCTCTTAC-3′, and the resulting clone (pSCUT12-1/M33*Nco*I) sequenced between the initiator codon and the *Hin*dIII site. A *Bgl*II–*Eco*RV fragment was subcloned back into the 4-kb genomic *cut12⁺* clone of pDCUT12-1 to form pDCUT12-1/M33*Nco*I. This construct was then digested with *Nco*I and *Pvu*II, which yields a 2.2-kb fragment bearing a truncated form of the *cut12⁺* gene encoding amino acids 33–548, along with ~300 bp 3′ of the gene, which was inserted into

pREP42-PkN. The regeneration of the full length *cut12*[+] gene from the truncated version in pREP42-PkN vector was complicated by the *Nde*I site that lies immediately upstream of the *Eco*RV site in pDCUT12-1. To circumvent this problem, a 1.6-kb *Nsi*I fragment that lacks the internal *Nde*I site was excised from pDCUT12–1/M33*Nde*I and cloned into the Bluescript plasmid to give pDCUT12-4. The 5′ region of the tagged truncated *cut12*[+] gene was then isolated from pREP42-PkN by *Nde*I–*Bgl*II digest, and the 0.5-kb fragment produced ligated to *Nde*I–*Bgl*II–digested pDCUT12-4. The *Nsi*I fragment from the resulting plasmid was then cloned back into pDCUT12-1, thereby generating a plasmid bearing the full length *cut12*[+] gene with two copies of the Pk epitope tag inserted at methionine 33, termed pDCUT12–1/M33Pk. The *Hin*dIII–*Eco*RV fragment from this plasmid was then cloned into *Hin*dIII–*Eco*RV–digested Bluescript with *ura4*[+] inserted at the *Not*I site to create the plasmid for integrative transformation of Pk-tagged *cut12*[+] into the genome, termed pINTCUT12-1/M33Pk.

Isolation of the stf1.1 *mutant locus by PCR and cloning PCR products*

The *stf1.1* mutant version of the *cut12*[+] gene was isolated by PCR amplification according to the protocol described for *cut12.1.* To clone the *stf1.1* mutant gene, a 0.5-kb *Nsi*I–*Bgl*II fragment was purified from the PCR product and ligated to *Nsi*I–*Bgl*II–digested pSCUT12-1/M1*Nde*I. The resulting clone was manually sequenced to confirm the presence of the *stf1.1* mutation in codon 71. To recreate full-length clones from this mutated construct, a *Bgl*II–*Eco*RV fragment was subcloned back into the 4-kb genomic *cut12*[+] clone, thereby regenerating a full-length *stf1.1* mutant version of *cut12*[+]. This construct was then digested with *Nde*I and *Pvu*II, to yield a 2.2-kb fragment bearing the full-length *cut12.G71V* cDNA and ~300 bp 3′ of the gene, which was cloned into *Nde*I–*Sma*I–digested pREP81.

Construction of GST–Cut12 fusion protein and antiserum production

A full-length *cut12*[+] with *Nde*I at M33 was digested with *Nde*I and *Pvu*II and cloned into the plasmid pGEX4T-3. This construct was transformed into the *Escherichia coli* strain BRL21 for the expression of GST–Cut12 fusion protein. Bacterially produced protein was eluted from a polyacrylamide gel by electrophoresis at 100 mÅ and dialysed against phosphate buffered saline. One hundred fifty micrograms of the resulting insoluble suspension of protein was mixed with complete Freund's adjuvant for the first injection, and incomplete Freund's adjuvant for two subsequent boosts. Antisera and affinity-purified sera were produced as described in Harlow and Lane (1988). Western blot detection was carried out with peroxidase conjugated anti-rabbit secondary antibody.

Fluorescence and immunofluorescence microscopy

For immunofluorescence microscopy, the procedures described by Hagan and Hyams (1988) were followed. The affinity purified anti-Sad1 antibody AP9.2 (Hagan and Yanagida 1995), anti-tubulin antibody TAT1 (Woods et al. 1989), and anti-Pk tag antibody 336 (Hanke et al. 1992) have been described previously. To improve microtubule preservation in cells double labeled with anti-tubulin and anti-Cut12, cells were mixed with an equal volume of prewarmed YES media plus 2.4 M sorbitol for 5 min prior to fixation in 4% paraformaldehyde. For the observation of GFP–Cut12 protein, cells were cultured in YES media, washed once in phosphate-buffered saline, and dried onto coverslips. GFP fusions were observed by use of Zeiss FITC set 10.

Electron microscopy

For electron microscopic localization of Cut12 and Pk antigens, samples were prepared by a modification of the methods of Ding et al. (1997). Briefly, cells were collected on a 0.45 µm millipore filter by vacuum filtration and were frozen in a Balzer's high pressure freezer (Balzers, Lichtenstein). Frozen samples were freeze-substituted on 0.1% gluteraldehyde in acetone at –90°C, warmed to –50°C, and embedded in Lowicryl HM20. Immunostaining was carried out as described previously (Demeter et al. 1995), by use of antibodies to Cut12 and Pk antigens followed by secondary antibodies conjugated to 10 and 5 nm of colloidal gold, respectively. Serial sections were imaged in a Philips CM10 electron microscope, negatives were digitized, and computer models were generated using the IMOD software package (Kremer et al. 1996).

References

Alfa, C.E., B. Ducommun, D. Beach, and J.S. Hyams. 1990. Distinct nuclear and spindle pole body populations of cyclin-cdc2 in fission yeast. *Nature* **347:** 680–682.

Bailly, E., M. Doree, P. Nurse, and M. Bornens. 1989. p34[cdc2] is located both in nucleus and cytoplasm; part is centrosomally associated at G2/M and enters vesicles at anaphase. *EMBO J.* **8:** 3985–3995.

Bailly, E., J. Pines, T. Hunter, and M. Bornens. 1992. Cytoplasmic accumulation of cyclin B1 in human cells: Association with a detergent resistant compartment and with the centrosome. *J. Cell Sci.* **101:** 529–545.

Balczon, R. 1996. The centrosome in animal cells and its functional homologs in plant and yeast cells. *Int. Rev. Cytol.* **169:** 25–82.

Barbet, N., W.J. Muriel, and A.M. Carr. 1992. Versatile shuttle vectors and genomic libraries for use with *Schizosaccharomyces pombe. Gene* **114:** 59–66.

Basi, G., E. Schmid, and K. Maundrell. 1993. TATA box mutations in the *Schizosaccharomyces pombe nmt1* promoter affect transcription efficiency but not the transcription start point or thiamine repressibility. *Gene* **123:** 131–136.

Belmont, L.D., A.A. Hyman, K.E. Sawin, and T.J. Mitchison. 1990. Real time visualization of cell cycle dependent changes in microtubule dynamics in cytoplasmic extracts. *Cell* **62:** 579–589.

Berry. L.D. and K.L. Gould. 1996. Novel alleles of *cdc13* and *cdc2* isolated as suppressors of mitotic catastrophe in *Schizosaccharomyces pombe. Mol. Gen. Genet.* **251:** 635–646.

Blangy, A., H.A. Lane, P. d'Herin, M. Harper, M. Kress, and E. Nigg. 1995. Phosphorylation by p34^{cdc2} regulates spindle association of human Eg5, a kinesin related motor essential for bipolar spindle formation in vivo. *Cell* **83:** 1159–1169.

Broek, D., R. Bartlett, K. Crawford, and P. Nurse. 1991. p34^{cdc2} is involved in establishing the dependence of S phase upon completion of the previous mitosis. *Nature* **349:** 388–393.

Buendia, B., G. Draetta, and E. Karsenti. 1992. Regulation of the microtubule nucleating activity of centrosomes in *Xenopus* egg extracts: Role of cyclin A-associated protein kinase. *J. Cell Biol.* **116:** 1431–1442.

Bueno, A. and P. Russell. 1993. Two fission yeast B-type cyclins Cig2 and Cdc13 have different functions in mitosis. *Mol. Cell. Biol.* **13:** 2286–2297.

Carr, A.M., S.A. MacNeill, J. Hayles, and P. Nurse. 1989. Molecular cloning and sequence analysis of mutant alleles of the fission yeast cdc2 kinase gene: Implications for cdc2 protein structure and function. *Mol. & Gen. Genet.* **218:** 41–49.

Coleman, T.R., Z. Tang, and W.G. Dunphy. 1993. Negative regulation of the wee1 protein kinase by direct action of the nim1/cdr1 mitotic inducer. *Cell* **72:** 919–929.

Demeter, J., M. Morphew, and S. Sazer. 1995. A mutation in RCC1-related protein pim1 results in nuclear envelope fragmentation in fission yeast. *Proc. Natl. Acad. Sci.* **92:** 1436–1440.

Den Haese, G.J., N. Walworth, A.M. Carr, and K.L. Gould. 1995. The Wee1 protein kinase regulates T14 phosphorylation of fission yeast cdc2. *Mol. Biol. Cell* **6:** 371–385.

Ding, R., K.L. McDonald, and J.R. McIntosh. 1993. Three dimensional reconstruction and analysis of mitotic spindles from the yeast *Schizosaccharomyces pombe. J. Cell Biol.* **120:** 141–151.

Ding, R., R.R. West, M. Morphew, B.R. Oakley, and J.R. McIntosh. 1997. The spindle pole body of *Schizosaccharomyces pombe* enters and leaves the nuclear envelope as the cell cycle proceeds. *Mol. Biol. Cell* **8:** 1461–1479.

Ducommun, B., G. Draetta, P. Young, and D. Beach. 1990. Fission yeast Cdc25 is a cell cycle regulated protein. *Biochem. Biophys. Res. Comm.* **167:** 301–309.

Dunphy, W.G. and A. Kumagai. 1991. The Cdc25 protein contains an intrinsic phosphatase activity. *Cell* **67:** 189–196.

Fantes, P. 1979. Epistatic gene interactions in the control of division in fission yeast. *Nature* **279:** 428–430.

Featherstone, C. and P. Russell. 1991. Fission yeast p107^{wee1} mitotic inhibitor is a tyrosine/serine kinase. *Nature* **349:** 808–811.

Gautier, J., M.J. Solomon, R.N. Booher, J.F. Bazan, and M.W. Kirschner. 1991. Cdc25 is a specific tyrosine phosphatase that directly activates p34^{cdc2}. *Cell* **67:** 197–211.

Glover, D.M., H. Ohkura, and A. Tavares. 1996. Polo kinase: The choreographer of the mitotic stage? *J. Cell Biol.* **135:** 1681–1684.

Gould, K.L. and P. Nurse. 1989. Tyrosine phosphorylation of the fission yeast *cdc2*$^+$ protein kinase regulates entry into mitosis. *Nature* **342:** 39–42.

Gould, K.L., S. Moreno, N.K. Tonks, and P. Nurse. 1990. Complementation of the mitotic activator, p80^{cdc25}, by a human tyrosine phosphatase. *Science* **250:** 1573–1576.

Gould, K. and A. Feoktistova. 1996. Characterization of novel mutations at the *Schizosaccharomyces pombe* cdc2 regulatory phosphorylation site, tyrosine 15. *Mol. Biol. Cell* **7:** 1573–1586.

Hagan, I.M. and J.S. Hyams. 1988. The use of cell division cycle mutants to investigate the control of microtubule distribution in the fission yeast *Schizosaccharomyces pombe. J. Cell Sci.* **89:** 343–357.

Hagan, I. and M. Yanagida. 1990. Novel potential mitotic motor protein encoded by the *cut7*$^+$ gene. *Nature* **347:** 563–566.

———. 1995. The product of the spindle formation gene *sad1*$^+$ associates with the fission yeast spindle pole body and is essential for viability. *J. Cell Biol.* **129:** 1033–1047.

———. 1997. Evidence for cell cycle specific, spindle pole body mediated, nuclear positioning in the fission yeast *Schizosaccharomyces pombe. J. Cell. Sci.* **110:** 1851–1866.

Hanke, T., P. Szawlowski, and R.E. Randall. 1992. Construction of solid matrix-antibody-antigen complexes containing simian immunodeficiency virus p27 using tag-specific monoclonal antibody and tag linked antigen. *J. Gen. Virol.* **73:** 653–660.

Harlow, E. and D. Lane. 1988. *Antibodies: A laboratory manual.* Cold Spring Harbor Laboratory, Cold Spring Harbor, NY.

Hayles, J., D. Fisher, A. Woollard, and P. Nurse. 1994. Temporal order of S phase and mitosis in fission yeast is determined by the state of the p34^{cdc2}–mitotic cyclin B complex. *Cell* **78:** 813–822.

Hoffmann, I., P.R. Clarke, M.J. Marcote, E. Karsenti, and G. Draetta. 1993. Phosphorylation and activation of human cdc25-C by cdc2-cyclin B and its involvement in the self amplification of MPF at mitosis. *EMBO J.* **12:** 53–60.

Horio, T., S. Uzawa, M.K. Jung, B. Oakley, K. Tanaka, and M. Yanagida. 1991. The fission yeast gamma tubulin is essential for mitosis and is localized to microtubule organizing centres. *J. Cell Sci.* **99:** 693–700.

Hudson, D. and P. Young. 1993. Sequence of the *Schizosaccharomyces pombe gtp1*$^+$ gene and identification of a novel family of putative GTP binding proteins. *Gene* **125:** 191–193.

Hudson, J.D., H. Feilotter, and P.G. Young. 1990. *stf1;* non-wee mutations epistatic to *cdc25* in the fission yeast *Schizosaccharomyces pombe. Genetics* **126:** 309–315.

Hudson, J.D., H. Feilotter, C. Lingner, R. Rowley, and P.G. Young. 1991. *stf1:* A new suppressor of the mitotic control gene *cdc25* in *Schizosaccharomyces pombe. Cold Spring Harbor Symp. Quant. Biol.* **56:** 599–604.

Hyman, A.A. and E. Karsenti. 1996. Morphogenetic properties of microtubules and mitotic spindle assembly. *Cell* **84:** 401–410.

Izumi, T. and J.L. Maller. 1993. Elimination of cdc2 phosphorylation sites in the cdc25 phosphatase blocks initiation of M-phase. *Mol. Biol. Cell* **4:** 1337–1350.

———. 1995. Phosphorylation and activation of the *Xenopus* cdc25 phosphatase in the absence of cdc2 and cdk2 kinase activity. *Mol. Biol. Cell* **6:** 215–226.

Izumi, T., D.H. Walker, and J.L. Maller. 1992. Periodic changes in phosphorylation of the *Xenopus* cdc25 phosphatase regulate its activity. *Mol. Biol. Cell* **3:** 927–939.

Kalt, A. and M. Schliwa. 1993. Molecular components of the centrosome. *Trends Cell Biol.* **3:** 118–128.

Kirschner, M. and T. Mitchison. 1986. Beyond self assembly: From microtubules to morphogenesis. *Cell* **45:** 329–342.

Kremer, J.R., D.N. Mastronarde, and J.R. McIntosh. 1996. Computer visualization of three-dimensional image data using IMOD. *J. Struct. Biol.* **116:** 71–76.

Kuang, J., C.L. Ashorn, M. Gonzalez-Kuyvenhoven, and J.E.

Penkala. 1994. cdc25 is one of the MPM-2 antigens involved in the activation of maturation promoting factor. *Mol. Biol. Cell* **5:** 135–145.

Kumagai, A. and W.G. Dunphy. 1991. The cdc25 protein controls tyrosine dephosphorylation of the cdc2 protein in a cell free system. *Cell* **64:** 903–914.

———. 1992. Regulation of the cdc25 protein during the cell cycle in *Xenopus* extracts. *Cell* **70:** 139–150.

———. 1996. Purification and molecular cloning of Plx1, a cdc25-regulatory kinase from *Xenopus* egg extracts. *Science* **273:** 1377–1380.

Labib, K., R.A. Craven, K. Crawford, and P. Nurse. 1995. Dominant mutants identify new roles of p34^{cdc2} in mitosis. *EMBO J.* **14:** 2155–2165.

Lane, H.A. and E.A. Nigg. 1996. Antibody microinjection reveals an essential role for human polo like kinase 1 (Plk1) in the functional maturation of mitotic centrosomes. *J. Cell Biol.* **135:** 1701–1713.

Lee, M.S., T. Enoch, and H. Piwnica-Worms. 1994. *mik1* encodes a tyrosine kinase that phosphorylates p34^{cdc2} on tyrosine 15. *J. Biol. Chem.* **269:** 30530–30537.

Lundgren, K., N. Walworth, R. Booher, M. Dembski, M. Kirschner, and D. Beach. 1991. Mik1 and wee1 cooperate in the inhibitory tyrosine phosphorylation of cdc2. *Cell* **64:** 1111–1122.

Lupas, A., M. v-Dyke, and J. Stock. 1991. Predicting coiled coils from protein sequences. *Science* **252:** 1102–1164.

MacNeill, S.A. and P. Nurse. 1993. Genetic analysis of human p34^{cdc2} function in fission yeast. *Mol. & Gen. Genet.* **236:** 415–426.

Maldonado-Codina, G. and D.M. Glover. 1992. Cyclins A and B associate with chromatin and the polar regions of spindles, respectively, and do not undergo complete degradation at anaphase in syncytial *Drosophila* embryos. *J. Cell Biol.* **116:** 967–976.

Masuda, H., M. Sevik, and W.Z. Cande. 1992. In vitro microtubule nucleating activity of spindle pole bodies in fission yeast *Schizosaccharomyces pombe:* Cell cycle dependent activation in *Xenopus* cell free extracts. *J. Cell Biol.* **117:** 1055–1066.

Maundrell, K. 1993. Thiamine repressible expression vectors pREP and pRIP for fission yeast. *Gene* **123:** 127–130.

McGowan, C.H. and P. Russell. 1995. Cell cycle regulation of human WEE1. *EMBO J.* **14:** 2166–2175.

Millar, J.B.A., G. Lenaers, and P. Russell. 1992. *Pyp3* PTPase acts as a mitotic inducer in fission yeast. *EMBO J.* **11:** 4933–4941.

Moreno, S., P. Nurse, and P. Russell. 1990. Regulation of mitosis by cyclic accumulation of p80^{cdc25} mitotic inducer. *Nature* **344:** 549–552.

Moreno, S., A. Klar, and P. Nurse. 1991. An introduction to the molecular genetic analysis in the fission yeast *Schizosaccharomyces pombe. Methods Enzymol.* **194:** 795–823.

Mueller, P.R., T.R. Coleman, and W.G. Dunphy. 1995. Cell cycle regulation of *Xenopus* wee1-like kinase. *Mol. Biol. Cell* **6:** 119–134.

Nigg, E. 1993. Cellular substrates of p34^{cdc2} and its companion cyclin dependent kinases. *Trends Cell Biol.* **3:** 296–301.

Nurse, P. 1975. Genetic control of cell size at cell division in yeast. *Nature* **256:** 547–551.

———. 1990. Universal control mechanisms regulating onset of M-phase. *Nature* **344:** 547–551.

Oakley, B.R. and N.R. Morris. 1983. A mutation in *Aspergillus nidulans* that blocks the transition from interphase to metaphase. *J. Cell Biol.* **96:** 1155–1158.

Ohkura, H., I.M. Hagan, and D.M. Glover. 1995. The conserved *Schizosaccharomyces pombe* kinase plo1, required to form a bipolar spindle, the actin ring, and septum, can drive septum formation in G$_1$ and G$_2$ cells. *Genes & Dev.* **9:** 1059–1073.

Ohta, K., N. Shiina, E. Okumura, S.I. Hisinaga, T. Kishimoto, S. Endo, Y. Gotoh, E. Nishida, and H. Sakai. 1993. Microtubule nucleating activity of centrosomes in cell free extracts from Xenopus eggs: Involvement of phosphorylation and accumulation of pericentriolar material. *J. Cell Sci.* **104:** 125–137.

Osmani, A.H., S.L. McGuire, and S.A. Osmani. 1991a. Parallel activation of the NIMA and p34^{cdc2} cell cycle regulated protein kinases is required to initiate mitosis in *A. nidulans. Cell* **67:** 283–291.

Osmani, A.H., K. O'Donnell, R.T. Pu, and S.A. Osmani. 1991b. Activation of the NIMA protein kinase plays a unique role during mitosis that cannot be bypassed by absence of the BIME checkpoint. *EMBO J.* **10:** 2669–2679.

Parker, L.L., S.A. Walter, P.G. Young, and H. Piwnica-Worms. 1993. Phosphorylation and inactivation of the mitotic inhibitor wee1 by the *nim1/cdr1* kinase. *Nature* **363:** 736–738.

Pichova, A., S.D. Kohlwein, and M. Yamamoto. 1995. New arrays of cytoplasmic microtubules in the fission yeast *Schizosaccharomyces pombe. Protoplasma* **188:** 252–262.

Pines, J. and T. Hunter. 1991. Human cyclins A and B1 are differentially located in the cell and undergo cell cycle dependent nuclear transport. *J. Cell Biol.* **115:** 1–17.

Pockwinse, S.M., G. Krockmalnic, S.J. Doxsey, J. Nickerson, J.B. Lian, A.J. van Wijen, J.L. Stein, G.S. Stein, and S. Penman. 1997. Cell cycle independent interaction of cdc2 with the centrosome, which is associated with the nuclear matrix intermediate filament scaffold. *Proc. Natl. Acad. Sci.* **94:** 3022–3027.

Russell, P. and P. Nurse. 1986. *cdc25$^+$* functions as an inducer in the mitotic control of fission yeast. *Cell* **45:** 145–153.

———. 1987a. Negative regulation of mitosis by *wee1$^+$*, a gene encoding a protein kinase homolog. *Cell* **49:** 559–567.

———. 1987b. The mitotic inducer *nim1$^+$* functions in a regulatory network of protein kinase homologs controlling the initiation of mitosis. *Cell* **49:** 569–576.

Saitoh, S., K. Takahashi, and M. Yanagida. 1997. Mis6, a fission yeast inner centromere protein, acts during G1/S and forms specialized chromatin required for equal segregation. *Cell* **90:** 131–143.

Sambrook, J., E.F. Fritsch, and T. Maniatis. 1989. *Molecular cloning: A laboratory manual* 2nd ed. Cold Spring Harbor Laboratory Press, Cold Spring Harbor, NY.

Sohrmann, M., S. Schmidt, I. Hagan, and V. Simanis. 1998. Asymmetric segregation on spindle poles of the *Schizosaccharomyces pombe* septum inducing protein kinase Cdc7p. *Genes & Dev.* **12:** 84–94.

Strausfeld, U., J.C. Labbe, D. Fesquet, J.C. Cavadore, A. Picard, K. Sadhu, P. Russell, and M. Doree. 1991. Dephosphorylation and activation of a p34^{cdc2}/cyclin B complex *in vitro* by a human CDC25 protein. *Nature* **351:** 242–245.

Tanaka, K. and T. Kanbe. 1986. Mitosis in the fission yeast *Schizosaccharomyces pombe* as revealed by freeze substitution electron microscopy. *J. Cell Sci.* **80:** 253–268.

Tang, Z., T.R. Coleman, and W.G. Dunphy. 1993. Two distinct mechanisms for negative regulation of the wee1 protein kinase. *EMBO J.* **12:** 3427–3436.

Verde, F., J.C. Labbe, M. Doree, and E. Karsenti. 1990. Regulation of microtubule dynamics by cdc2 protein kinase in cell free extracts of *Xenopus* eggs. *Nature* **343:** 233–238.

Verde, F., M. Dogterom, E. Stelzer, E. Karsenti, and S. Leibler. 1992. Control of microtubule dynamics and length by cyclin A and cyclin B dependent protein kinases in *Xenopus* egg extracts. *J. Cell Biol.* **118:** 1097–1108.

Watanabe, N., M. Broome, and T. Hunter. 1995. Regulation of the human Wee1Hu CDK tyrosine 15-kinase during the cell cycle. *EMBO J.* **14:** 1878–1891.

Westendorf, J.M., P.N. Rao, and L. Gerace. 1994. Cloning of cDNAs for M phase phosphoproteins recognized by the MPM2 monoclonal antibody and determination of the phosphorylated epitope. *Proc. Natl. Acad. Sci.* **91:** 714–718.

Woods, A., T. Sherwin, R. Sasse, T.H. MacRae, A.J. Baines, and K. Gull. 1989. Definition of individual components within the cytoskeleton of *Trypanosoma brucei* by a library of monoclonal antibodies. *J. Cell Sci.* **93:** 491–500.

Wu, L. and P. Russell. 1993. Nim1 kinase promotes mitosis by inactivating Wee1 tyrosine kinase. *Nature* **363:** 738–741.

Ye, X.S., G. Xu, P.T. Pu, R.R. Fincher, S.L. McGuire, A.H. Osmani, and S.A. Osmani. 1995. The NIMA protein kinase is hyperphosphorylated and activated downstream of p34^{cdc2}/cyclin B: Coordination of two mitosis promoting kinases. *EMBO J.* **14:** 986–994.

Ye, X.S., R.R. Fincher, A. Tang, K O'Donnell, and S.A. Osmani. 1996. Two S phase checkpoint systems, one involving the function of both BIME and Tyr15 phosphorylation of p34^{cdc2}/cyclin B, inhibit NIMA and prevent premature mitosis. *EMBO J.* **15:** 3599–3610.